Microelectronics Reliability 79 (2017) 314–320

Contents lists available at ScienceDirect

Microelectronics Reliability

journal homepage: www.elsevier.com/locate/microrel

In situ tensile testing of tin (Sn) whiskers in a focused ion beam (FIB)/scanning electron microscope (SEM)

Renuka Vallabhaneni [a], Ehsan Izadi [b], Carl R. Mayer [a], C. Shashank Kaira [a], Sudhanshu S. Singh [a,c], Jagannathan Rajagopalan [a,b], Nikhilesh Chawla [a,b,*]

[a] Materials Science and Engineering, Arizona State University, Tempe, AZ 85287-6106, USA
[b] Mechanical Engineering, Arizona State University, Tempe, AZ 85287-6106, USA
[c] Department of Materials Science and Engineering, Indian Institute of Technology, Kanpur, Uttar Pradesh 208016, India

ARTICLE INFO

Article history:
Received 22 May 2017
Received in revised form 7 July 2017
Accepted 8 July 2017
Available online 19 July 2017

Keywords:
Tin whiskers
Tensile strength
In situ
FIB/SEM

ABSTRACT

Tin and tin-alloyed electroplated films are known to be susceptible to whisker growth under a range of conditions, many of which result in the generation of compressive stresses in the film. Compressive stress is considered to be one of the primary causes for whisker nucleation and growth. While extensive investigations have been performed on whisker growth, there have been few studies on the mechanical properties of tin whiskers themselves. We report on the tensile behavior of tin whiskers that were obtained by indentation and furnace aging of electroplated tin films on copper disks. Tensile tests of the whiskers were conducted *in situ* in a dual beam focused ion beam (FIB)-scanning electron microscope (SEM) system using a micro electro-mechanical systems (MEMS) based tensile testing stage. The strength of the whiskers was found to decrease with an increase in gage length and aged whiskers were found to be weaker than their indented counterparts. The observed gage length effect can be attributed to the probability of finding more defects as the whisker length increases. The effect of processing on the observed strength variation was investigated by analyzing the oxygen content in the whiskers *via* energy dispersive spectroscopy and the microstructure through transmission electron microscopy (TEM). The deformation mechanisms of whiskers were also inferred using post-mortem TEM. It was observed that the whiskers grown by indentation were dislocation free both before and after deformation. In contrast, whiskers grown by aging showed notable dislocation content (arranged in low energy configurations) even before deformation.

1. Introduction

Restricted usage of Pb in electronic products due to its toxicity has resulted in electronic suppliers moving towards the usage of pure Sn or Sn-based alloys [1]. However, the usage of pure Sn and high Sn content based coatings, without Pb, has resulted in a reliability concern regarding the formation of conductive tin whiskers. These tin whiskers are thin filaments known to grow spontaneously from Sn which can lead to short-circuits and system failures [2]. Hence, an understanding of the properties of tin whiskers and growth mechanisms is important.

While the exact mechanisms for whisker nucleation and growth are still being studied, there is a consensus that compressive stresses are necessary for their formation [3–5]. Compressive stresses can be induced by mechanical, chemical, and thermal effects [6]. These can be internal stresses arising due to various reasons such as residual (or plating) stress [7–9], intermetallic growth [10–14], oxidation and corrosion [15], *etc.* all of which result in whisker formation. Compressive stress can also be induced by external pressure, which was also found to accelerate the growth of Sn whiskers [16].

Even though the phenomenon of Sn whiskering has been studied for decades, little is known about the mechanical properties of the whiskers themselves. Very few studies have been conducted on the mechanical behavior of Sn whiskers owing to the difficulties of handling, gripping, and testing such fine-diameter and high-aspect-ratio whiskers [17]. Powell and Skove [18] performed tensile tests on tin whiskers and obtained force *versus* displacement curves, but the strength was not reported. Dunn [19] attempted to obtain bending stiffness of Sn whiskers and reported Young's modulus values with large variability. Manual handling of whiskers, assumption of a circular cross-section, and errors due to optical microscopy based measurement of whisker diameters in these previous studies have resulted in significant experimental uncertainty. Therefore, more precise experimental techniques are required to evaluate the mechanical properties of whiskers. Recently, Singh et al. [17] utilized a novel method for *in situ* focused ion beam (FIB)-scanning electron microscope (SEM) testing of tin whiskers using a micro-electro-mechanical systems (MEMS) testing device. This

* Corresponding author at: Materials Science and Engineering, Arizona State University, Tempe, AZ 85287-6106, USA.
E-mail address: nchawla@asu.edu (N. Chawla).

http://dx.doi.org/10.1016/j.microrel.2017.07.042
0026-2714/

method of testing provides much more accurate and reliable results than previously possible. This is because the MEMS testing device provides higher load and displacement resolution, while the FIB cross sectioning allows for high-resolution measurement of the whisker area required for accurate stress determination. Additionally, the possible damage associated with manual handling is eliminated by using an *in situ* micromanipulator.

In this work, we have conducted an in-depth study of the tensile behavior of whiskers prepared by two different techniques: indentation and high temperature furnace aging. The sources of compressive stress and the grain structures were investigated in each of these cases. The whiskers were then tested *in situ* in a FIB-SEM at two different gage lengths: 20 μm and 50 μm utilizing a MEMS tensile testing stage. An attempt was made to understand the effect of gage length and method of processing on the strength of whiskers. To understand the effect of processing on the strength of the whiskers, the possibility of difference in oxygen contents on the two types of samples was investigated and subsequent TEM analysis was conducted. Possible mechanisms of deformation in tin whiskers from the TEM results are also discussed.

2. Materials and experimental procedure

Oxygen-free Cu rod (alloy 101, Rockwell F84–94, 9.5 mm diameter) was cut into 3 mm thick disks with an electric discharge machine (EDM) to use as the Sn plating substrate. These were then ground and polished to a 0.05 μm finish. After polishing, the disk was ultrasonically cleaned in ethanol and dried before being placed in the electrolytic cell. The Cu disc was used as the cathode, and a Sn strip, polished and cleaned in a similar manner, was used as the anode. The initial objective of this work was to grow whiskers on these electroplated samples so that these whiskers could be used for testing and further analysis. Since it is known that bright Sn plating has more propensity for whisker formation [20,21], a sulfate based electrolyte with commercial brightening agents (Electrochemical Products Inc., E-Brite 180) was used. A thin (less than 5 μm) layer of electrodeposited Sn was preferred since it has been noted by others [22–24] that thicker coatings tend to have fewer whiskers. Plating was achieved in a vertical polytetrafluoroethylene (PTFE) reactor with cathode current density of 212 A/m^2 for 5 min. Based on profilometry (Bruker Dektak XT) measurements, the thickness of the Sn plated films was found to be about 2 μm. After plating, the samples were given a light polish to ensure minimum damage to the Sn film surface.

Sn whisker formation and growth has been shown to be mainly a stress relief phenomenon [14,25–30,31]. Accelerated whisker growth in this study was achieved by the introduction of compressive force in the Sn film by two different methods: Indentation and high temperature furnace aging. To relieve this compressive stress induced in the tin film, formation of tin whiskers and hillocks (low aspect ratio whiskers) has been observed.

The samples were indented for a period of 3 days with a custom-made indentation apparatus consisting of 300 g weight and a tungsten-carbide ceramic ball as described elsewhere [32]. Another set of Sn plated samples were aged at 100 °C in a laboratory furnace for about 30 days. Both the indented and aged samples were checked periodically in a SEM (JEOL JSM-6100 SEM) for whisker and hillock growth. FIB cross-sectioning was performed on both types of samples to understand the sources of stress and the underlying mechanisms for whisker/hillock growth. A dual-beam FIB-SEM (Nova 200 NanoLab FEGSEM/FIB, FEI Co, Oregon) was used in this study. Cross-sectioning was performed by milling a trench starting with a current of 7 nA and subsequent polishing of the cross-sectioned surface using finer currents until a current of 50 pA. Ion-channeling imaging was also performed in the cross-section to reveal the grain structure.

The whiskers obtained by the above-mentioned methods were utilized for testing. Straight whiskers were chosen and their initial area was measured by the cross-section of the whisker tip, imaging using FIB-SEM and later correcting this image for the 52° angle at which it was taken. The area was obtained by manual outlining using the image-processing software (ImageJ, Bethesda, MD) and image segmentation was conducted to accurately quantify the actual cross-sectional area of the whisker (Fig. 1).

Since the whisker needed to be placed on the MEMS device for testing, trenches of appropriate dimensions matching the dimensions of the whisker were milled on the MEMS device for the whisker. Initial cross-sectioning of the whisker for area calculations also helped in knowing the dimensions of the whisker precisely and the trenches were milled accordingly using the FIB. Small fiduciary marks were also made on the device, on the side of the trenches, in order to track the load and displacement during the experiment. The process by which Sn whiskers were tested in this study is similar to that of Singh et al. [17] and is shown in Fig. 2. A tungsten needle was welded to a Sn whisker in FIB/SEM by depositing platinum to attach the needle and the whisker (Fig. 2(a)). The ion beam was then used to cut the Sn whisker (Fig. 2(b)). The needle was moved to the trench in the MEMS device, and Pt was again used to weld the whisker in the trenches. The ion beam was then used to cut the needle from the whisker (Fig. 2(c), (d)).

After welding, the whisker was deformed in a quasi-static manner by loading the MEMS stage using a piezo actuator with a displacement resolution of approximately 30 nm. The MEMS stage, which is very similar to stages previously used to test freestanding thin films [33,34], was fabricated using the process described elsewhere [35,36]. The stage has built-in force and displacement sensors which allow simultaneous measurement of stress and strain in the whisker during *in situ* deformation. Alignment beams and U-springs ensure alignment of the sample with the loading axis while maintaining the structural integrity of the device. Precision alignment of the whisker in the MEMS stage resulted in accurate measurement of the stress–strain behavior. Furthermore, the MEMS

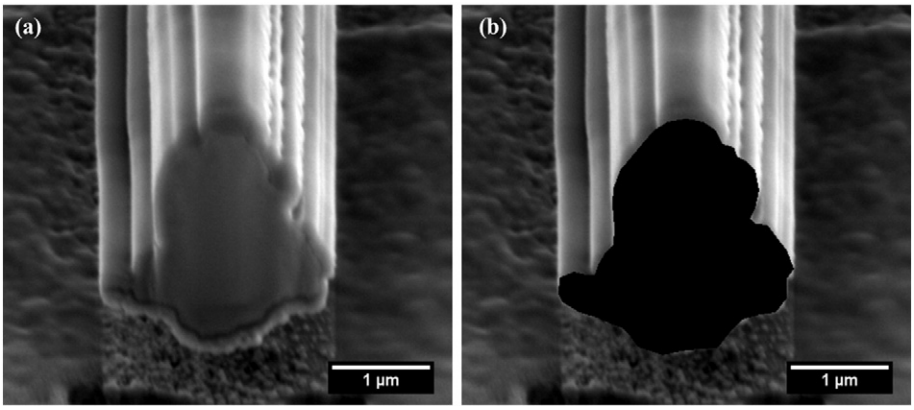

Fig. 1. Measurement of cross-sectional area: (a) Whisker cross-section, (b) selection of the region in Image J.

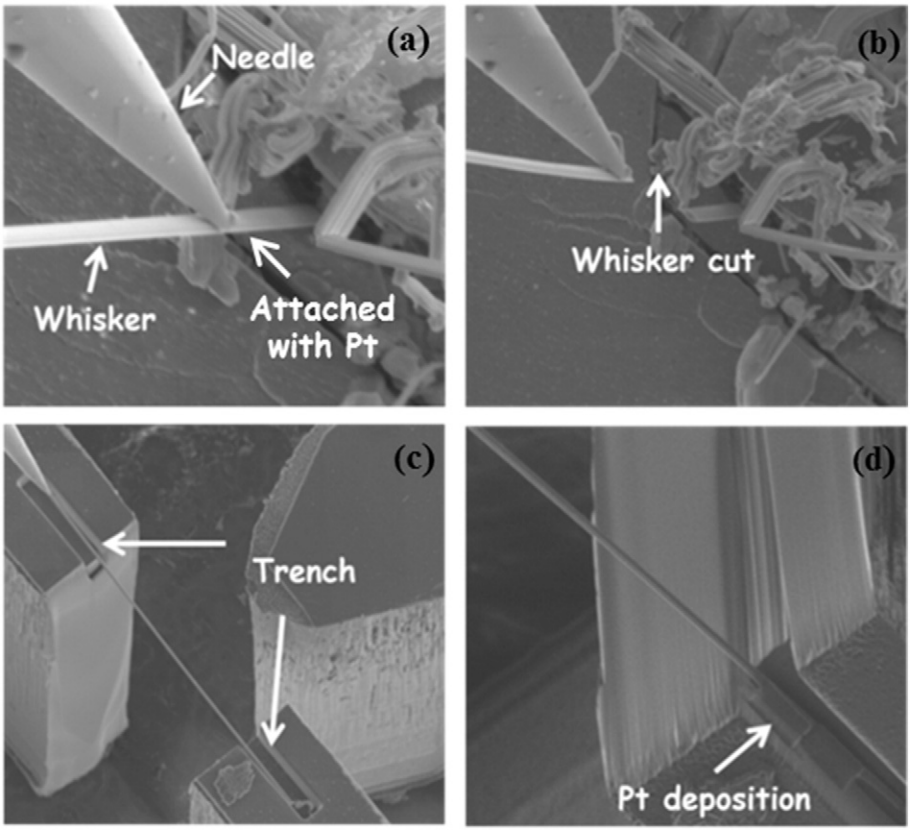

Fig. 2. Process of whisker lift-out and placement on the device inside the FIB/SEM: (a) Needle touching the whisker and welding of the whisker to the needle using platinum, (b) Cutting the whisker near welded region using FIB, (c) Placement of Sn whisker inside the trenches made in the MEMS device and (d) The whisker is welded in place using Pt in both the trenches.

stage is designed to ensure uniform uniaxial loading of the whisker and to minimize any bending or torsion that could arise from loading misalignment [37]. During testing, one end of the MEMS stage was fixed and displacement was imposed on the other end, in increments of about 150 nm, by gradually increasing the voltage on the piezo. After each loading step, the elongation and force on the whisker were recorded. This process was repeated until the whisker fractured. The elongation and force on the whisker were used to calculate the strain and stress on the whisker using its length and initial cross-sectional area.

To study the oxygen content variation with the processing method and relate it to the strength of whiskers, a qualitative comparison using energy dispersive spectroscopy (EDS) in an electron microprobe (JXA-8530F, JEOL) was conducted on both indented and aged samples. TEM samples were prepared using the FIB lift-out technique to understand the deformation mechanisms. These samples were made from both as-grown whiskers as well as deformed whiskers of both types. A part of the whisker was cut using FIB and lifted-out using an *in situ* nanomanipulator to place it on a standard TEM Cu grid. This was later thinned down to electron transparency using a fine current at an accelerating voltage of 10 keV. Thinning was carried out in two ways such that samples were made along the growth direction of the whisker and also perpendicular to it (cross-section).

3. Results and discussion

Fig. 3(a) shows the top view of the electroplated Sn film compressed for 3 days with the indenter described previously. Whiskers were observed at the boundary between the deformed region (by the ball

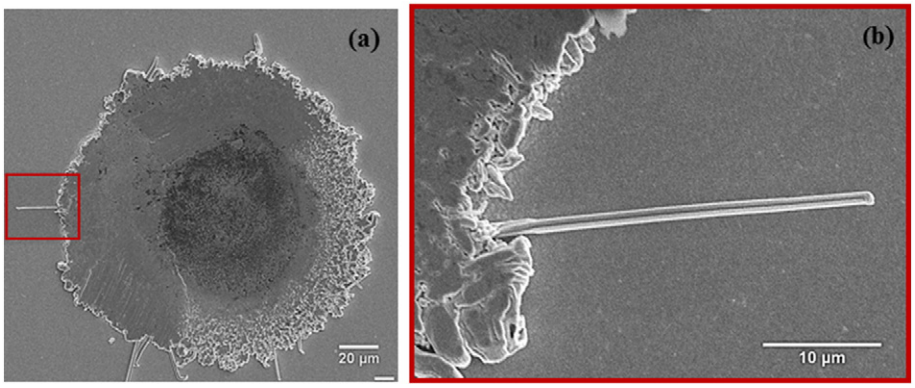

Fig. 3. (a) Top view of an indent showing whiskers at the boundary between deformed and un-deformed region and (b) Magnified image of a whisker obtained by the method of indentation.

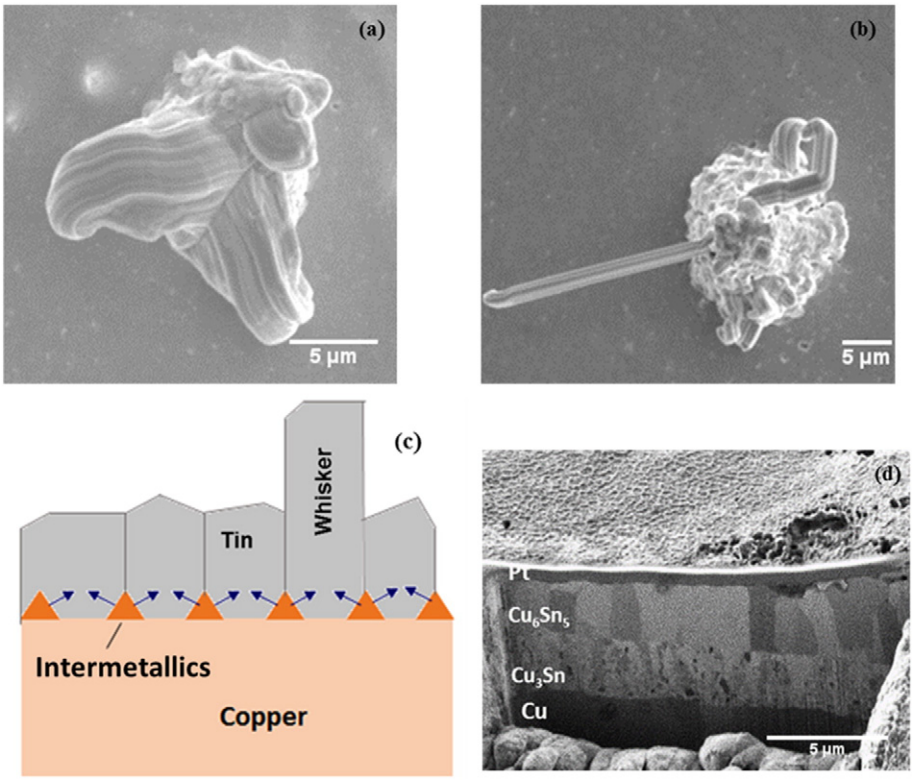

Fig. 4. Whiskers and hillocks on aged sample: (a) Hillock, (b) Whisker from the hillock, (c) Schematic showing intermetallic formation at Cu-Sn interface and (d) FIB cross-sectional image after ion-channeling of an aged sample showing two distinct intermetallic layers of Cu_6Sn_5 and Cu_3Sn.

indenter) and the un-deformed region. Fig. 3(b) represents a magnified view of one such whisker. Typically, whiskers obtained using this method were 10–70 μm long and 0.6–3 μm thick. Similar results were obtained by Doudrick et al. [32] and Williams et al. [38] who observed whiskers and hillocks, respectively by indentation. FIB cross-section followed by ion channeling imaging was performed in the un-deformed region as well as the deformed region of the Sn plating.

Fig. 4(a) and (b) shows Sn whiskers and hillocks obtained by aging the electroplated samples at high temperature (100 °C). Typically, hillocks were observed after about 10 days of aging and the density of these hillocks increased with aging time. Most whiskers were found to form from these hillocks after about 20 days of aging, with very few whiskers forming directly from the Sn plated surface. The protrusion of whiskers from hillocks was observed as a result of the tendency to reduce the surface-free energy of hillocks [39].

Typically, whiskers obtained by high temperature furnace aging were 10 μm–280 μm long and 1 μm–10 μm thick. Cu-Sn intermetallic compound formation at the Sn/Cu interface is likely to be one of the primary reasons behind introduction of compressive stress in aged samples. This compressive stress in Sn is thought to be due to the volume increase by the growth of the intermetallic compounds [40] (Fig. 4(c)). Extensive intermetallic growth was observed in the aged samples as shown in Fig. 4(d) with two distinct, uniform layers of Cu-Sn intermetallic compounds namely, Cu_6Sn_5 and Cu_3Sn.

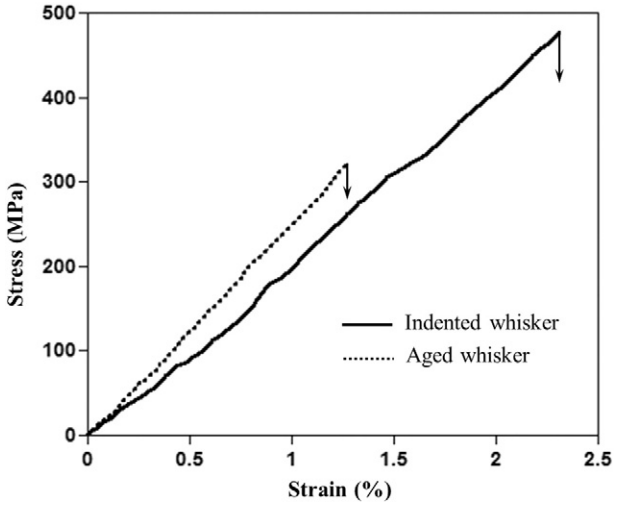

Fig. 5. Representative tensile stress-strain curves of indented and aged whiskers. These whiskers were tested with a gage length of 50 μm and the area measured was about 2 μm^2.

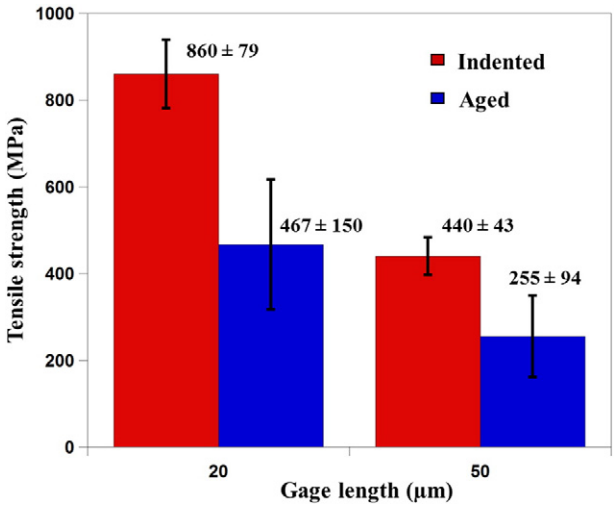

Fig. 6. The effect of gage length and processing on the strength of whiskers.

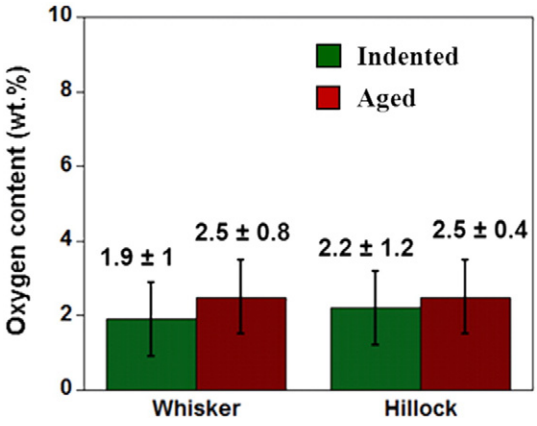

Fig. 7. EDS analysis showing the variation of oxygen content on whiskers and hillocks.

Striations were observed on the surface of most whiskers obtained by both the methods giving the appearance of having been extruded from the surface [41,42]. These groves are found to be parallel to the growth axis of the whiskers.

Tin whiskers have a much higher strength compared to bulk tin because of the much lower defect density in the whisker. Whiskers of similar diameter were tested and multiple whiskers tested at each condition produced similar strength values indicating the reliability and repeatability of the testing method. The stress-strain curves for both annealed and indentation-induced whiskers were fairly linear till failure (Fig. 5).

The strength of the whiskers decreased with an increase in gage length, *i.e.*, for a particular type of whisker, the strength of the whiskers with 50 μm gage length was lower strength than those with 20 μm gage length, as shown in Fig. 6. One possible explanation for this observed strength difference is the flaw-dependent nature of fracture in these materials. In smaller volumes of material there is a lower probability of the material containing a strength limiting flaw, leading to a much higher strength. In addition, at a particular gage length, it was observed that the whiskers obtained by high temperature furnace aging showed lower strength than the whiskers obtained by indentation as shown in Fig. 6. This indicates that the behavior of whiskers is dependent on the growth mechanism. Possible explanations for the lower strength of whiskers obtained by high temperature aging are discussed in the following sections.

One of the potential causes for the observed processing effect on the strength of whiskers is the possibility of higher oxygen content in the whiskers obtained by high temperature aging. From the EDS analysis (Fig. 7), it can be seen that the oxygen content on whiskers and hillocks was similar for both processing methods. The oxygen content on the whiskers and hillocks obtained by indentation at room temperature was around 2 wt%. Even after aging at high temperature (100 °C) for about 30 days, the oxygen content did not vary much and remained in the similar range. This indicates that the tin oxide formed initially is tenacious and the rate of tin oxide growth is not significant upon exposure to elevated temperatures as shown by others [43]. Based on this result, the lower strength of aged whiskers cannot be attributed to greater oxidation.

To resolve this issue, TEM analysis was conducted on both as-grown and deformed Sn whiskers obtained using both aging and indentation. The as-grown whiskers obtained from indentation were found to be free of defects, as shown in Fig. 8(a). Post-mortem TEM characterization also showed an absence of stored dislocations in fractured whiskers (Fig. 8(b)).

The as-grown aged whiskers showed dislocations arranged in the form of ordered arrays (Fig. 9(a), (b)). The aged whiskers were exposed to high temperatures for a prolonged period of time prior to the test, which could facilitate the climb and cross-slip of dislocations, and eventual rearrangement into low-energy configurations (boundaries), resulting in the ordered array structure. An increased density of the dislocations along with extensive development of cell-like structures was seen in the deformed aged whiskers (Fig. 9(c)–(f)). When subjected to load, the dislocations behaved very similar to bulk tin forming subgrains. Cross slip, climb can occur easily facilitating their formation. It is also possible that several of these boundaries try to link together (Fig. 9 (c)) and result in the formation of sub-grain structures (Fig. 9(e), (f)). The constituent dislocations at the sub-grain boundary can be clearly seen in Fig. 9(d). Similar sub-grain structure in the present study was also observed in bulk electrodeposited tin coatings upon the application stress [14,29]. The sub-grain formation is an indication of dynamic recovery, a phenomenon commonly observed in metals being plastically deformed at temperatures around (0.5–0.7) T_m [29].

On the other hand, the indentation-induced whiskers were free of any dislocations in the as-processed condition. Thus, nucleating a dislocation requires very high stress resulting in a very high strength. Deformation proceeding by the requirement of nucleation of new dislocations resulting in high strengths has been reported in numerous studies. Julia R. Greer et al. showed hardening by dislocation starvation in submicrometer sized gold crystals [44]. They observed high strengths of gold pillars, about 50 times stronger than that of their bulk counterparts. This was attributed to dislocation annihilation at free surfaces thereby reducing overall dislocation multiplication rate leading to a dislocation starved state and requiring high strengths to nucleate new dislocations. Z. W. Shan et al. [45] showed mechanical annealing of defects in sub micrometer Ni pillars and showed that atypical hardening and high strengths in these is controlled by the activation of new dislocation sources.

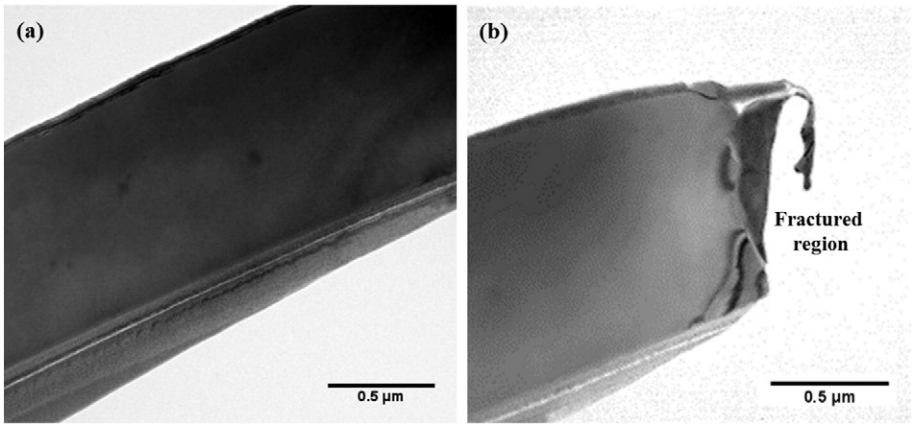

Fig. 8. (a, b) Bright field TEM images of deformed Sn whiskers obtained by indentation showing absence of dislocation storage.

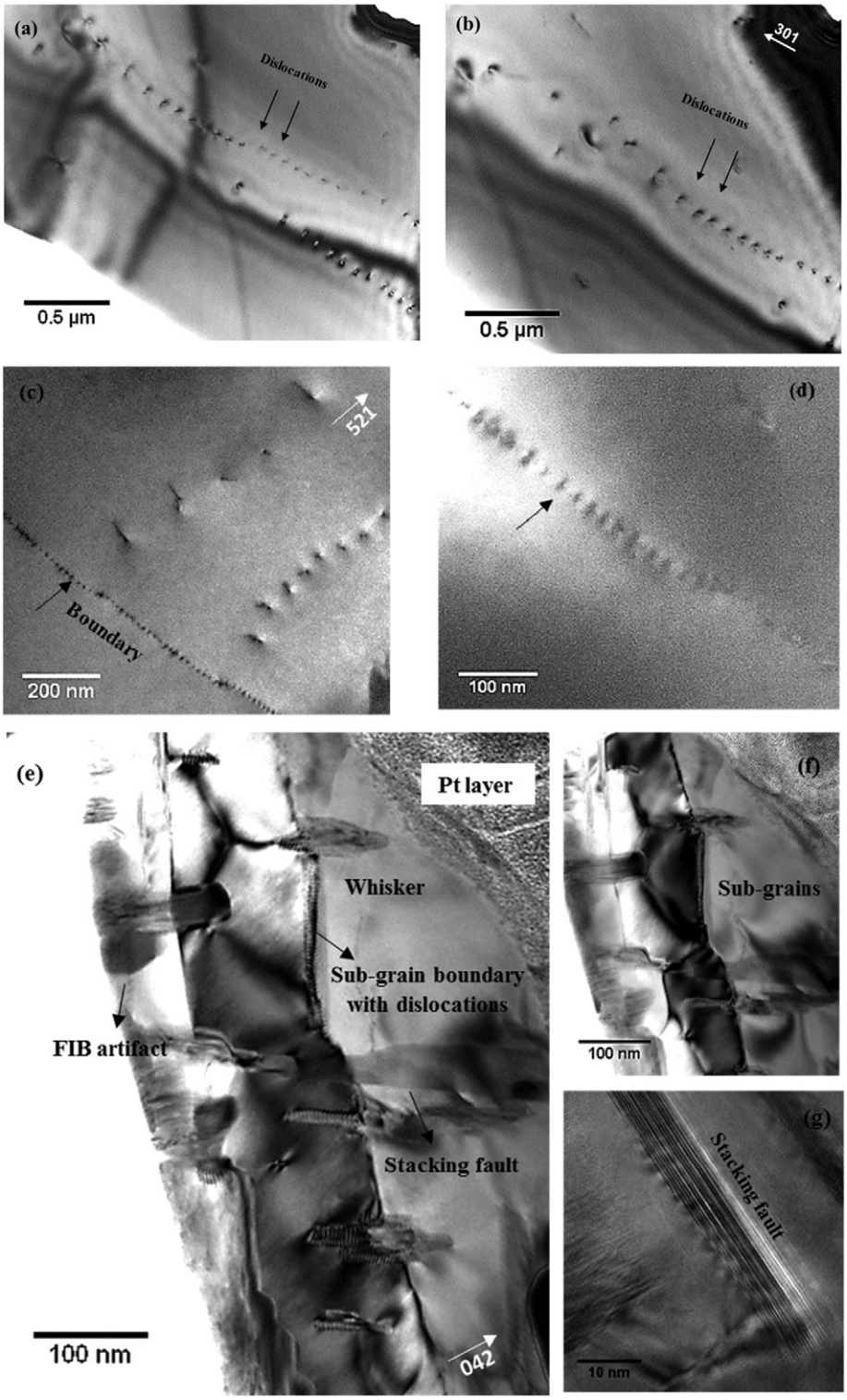

Fig. 9. Bright field TEM images of Sn whiskers obtained by high temperature furnace aging: (a, b) As-grown whiskers showing dislocation array structure (c) Deformed whisker showing low energy boundaries trying to link up to form sub-grains (d) Individual dislocations of a sub-grain boundary shown in c (e) Deformed whisker showing sub-grain boundaries with the constituent dislocations and stacking faults emanating from the sub-grain boundaries (f) Clear view of some of the sub-grains shown in (e) (g) Stacking fault observed in a deformed whisker.

Apart from sub-grains, stacking faults with a fringe like appearance were also observed in aged whiskers emanating from sub-grain boundaries as shown in Fig. 9(e) and (g). Dislocations from the sub-grain boundaries might be emitted leaving behind a stacking fault. It was interesting to observe stacking faults in tin whiskers evidencing partial dislocation activity although tin is a high stacking fault energy material. The existence of partial dislocations in Sn has been corroborated by both simulation and experimental studies. Kinoshita et al. [46] performed simulations to study the energetically favorable slip paths of slip systems in Sn and suggested that it is energetically favorable for dislocations to dissociate on certain slip systems in tin. C. Shashank Kaira [47] et al. performed TEM analysis on a deformed bicrystal Sn

micropillar and observed partial dislocation activity at the vicinity of a twin boundary.

The contrasting features observed in the two types of whiskers lead to the conclusion that the structure and, hence, the mechanical behavior of tin whiskers differs significantly with the growth mechanism because of changes in initial microstructure. The strength variation observed between the indented and aged whiskers in this study could be understood by the fact that the stress required to move pre-existing dislocations in aged whiskers is lower than that required for dislocation nucleation in indentation-induced whiskers.

4. Summary

In the present study, tin whiskers were obtained for tensile tests using two accelerated growth methods: indentation and high temperature furnace aging. Both methods introduce compressive stress in the electroplated Sn film and whiskers were found to nucleate and grow to relieve this stress.

1. Tensile tests were carried out by lifting out whiskers using FIB and placing them on MEMS tensile testing stage inside FIB-SEM. Multiple whiskers tested at each condition produced similar strength values indicating the reliability and repeatability of the testing method. It was observed that the tin whiskers possess high strengths due to their low defect densities compared to bulk tin.
2. The strength of the whiskers was found to be dependent on the gage length and the processing method. Since there is a high probability to encounter defects as the length is increased, the strength of the whiskers was found to decrease with an increase in their length. EDS analysis indicated that oxide growth is not significant in whiskers even at relatively high temperature (100° C) hence the lower strength of the aged whiskers cannot be attributed to oxygen incorporation.
3. TEM analysis was performed to understand the processing effect as well as the deformation mechanisms in tin whiskers. It is evident from the TEM results that the deformation in the indented whiskers is controlled by dislocation nucleation, which explains their high strengths. In contrast, deformation in the aged whiskers is mainly controlled by the rearrangement of dislocations into low-energy configurations and formation of sub-grains, similar to the behavior of bulk tin. These differences in microstructural features observed in the two types of whiskers can explain the strength variation observed.

Acknowledgements

The authors are grateful for financial support from the Air Force Office of Scientific Research (AFOSR) FA9550-14-1-0073 (Drs. J. Tiley and A,. Sayir, Program Managers) through the MURI Program. We acknowledge the use of facilities within the Leroy Eyring Center for Solid State Science at Arizona State University.

References

[1] iNEMI Tin Whisker User Group, Recommendations on lead-free finishes for components used in high-reliability products, version 4, http://www.inemi.org/cms/ (accessed 04/15/2016).
[2] NASA, Multiple examples of whisker-induced failures are documented on the NASA website, http://nepp.nasa.gov/whisker/ (accessed 04/15/2016).
[3] R.M. Fisher, L.S. Darken, K.G. Carroll, Acta Metall. 2 (1954) 368–369 (371-373).
[4] B.D. Dunn, Circuit World 2 (1976) 32–40.
[5] Chen Xu, Yun Zhang, Chonglun Fan, J.A. Abys, IEEE Trans. Electron. Packag. 28 (2005) 31–35.
[6] W.J. Choi, T.Y. Lee, K.N. Tu, N. Tamura, R.S. Celestre, A.A. Mcdowell, et al., Proceedings of the 52nd Electronics Components and Technology Conference; May 28–31, 2002 628–633.
[7] M. Sobiech, C. Krüger, U. Welzel, J.Y. Wang, E.J. Mittemeijer, W. Hügel, J. Mater. Res. 25 (2010) 2166–2174.
[8] M.J. Bozack, E.R. Crandall, C.L. Rodekohr, R.N. Dean, G.T. Flowers, J.C. Suhling, IEEE Trans. Electron. Packag. Manuf. 33 (2010) 198–204.
[9] K. Murakami, M. Okano, M. Hino, M. Takamizawa, K. Nakai, Mater. Trans. 51 (2010) 143–151.
[10] W.J. Boettinger, C.E. Johnson, L.A. Bendersky, K.W. Moon, M.E. Williams, G.R. Stafford, Acta Mater. 53 (2005) 5033–5050.
[11] K.N. Tu, Acta Metall. 21 (1973) 347–354.
[12] X. Deng, G. Piotrowski, J.J. Williams, N. Chawla, J. Electron. Mater. 32 (2003) 1403–1413.
[13] B.Z. Lee, D.N. Lee, Acta Mater. 46 (1998) 3701–3714.
[14] E. Chason, N. Jadhav, W.L. Chan, L. Reinbold, K.S. Kumar, Appl. Phys. Lett. 92 (2008) 171901.
[15] Craig Hillman, Gregg Kittlesen, Randy Schueller, A new (better) approach to tin whisker mitigation, Dfr solutions, http://www.dfrsolutions.com/uploads/white-papers/WP_SnWhisker.pdf (accessed 04/15/2016).
[16] Tadahiro Shibutani, Qiang Yu, Masaki Shiratori, Michael G. Pecht, Microelectron. Reliab. 48 (2008) 1033–1039.
[17] S.S. Singh, R. Sarkar, H.-X. Xie, C. Mayer, J. Rajagopalan, N. Chawla, J. Electron. Mater. 43 (2014) 978–982.
[18] B.E. Powell, M.J. Skove, J. Appl. Phys. 36 (1965) 1495–1496.
[19] B.D. Dunn, Eur. Space Agency (ESA), Report STR-223, 1987 1–51.
[20] NASA, The continuing dangers of tin whiskers and attempts to control them with conformal coating, http://nepp.nasa.gov/docuploads/95565195-0E5A-40D8-98D88425FF668F68/JayBrusseRevision2.pdf (accessed 04/15/2016).
[21] Joe Smetana, iNEMI tin whisker user group IPC/APEX, Recommendations on lead-free finishes for components used in high-reliability products, http://thor.inemi.org/webdownload/newsroom/Presentations/APEX_2006/S04%20Tin%20Whiskers/iNEMI_Recommendations_Tin%20whisker%20mitigation_APEX06.pdf February 2006 (accessed 04/15/2016).
[22] L.A. Pinol, J. Melngailis, H.K. Charles, D.M. Lee, R. Deacon, G. Coles, G. Clatterbaugh, IEEE Trans. Compon. Packag. Manuf. Technol. 1 (2011) 2028–2032.
[23] J. Cheng, F.Q. Yang, P.T. Vianco, B. Zhang, J.C.M. Li, J. Electron. Mater. 40 (2011) 2069–2075.
[24] M.H. Lu, K.C. Hsieh, J. Electron. Mater. 36 (2007) 1448–1454.
[25] S.C. Britton, Trans. Inst. Met. Finish. 52 (1974) 95–102.
[26] W.J. Choi, T.Y. Lee, K.N. Tu, N. Tamura, R.S. Celestre, A.A. MacDowell, Y.Y. Bong, L. Nguyen, Acta Mater. 51 (2003) 6253–6261.
[27] K.N. Tu, Phys. Rev. B 49 (1994) 2030–2034.
[28] B.-Z. Lee, D.N. Lee, Acta Mater. 46 (1998) 3701–3714.
[29] K.S. Kumar, L. Reinbold, A.F. Bower, E. Chason, J. Mater. Res. 23 (2008) 2916–2934.
[30] J.W. Osenbach, J.M. De Lucca, B.D. Potterger, A. Amin, R.L. Shook, F.A. Baiocchi, IEEE Trans. EPM 30 (2007) 23–35.
[31] W.J. Boettinger, C.E. Johnson, L.A. Bendersky, K.-W. Moon, M.E. Williams, G.R. Stafford, Acta Mater. 53 (2005) 5033–5050.
[32] Kyle Doudrick, Jeff Chinn, Jason Williams, Nikhilesh Chawla, Konrad Rykaczewski, Microelectron. Reliab. 55 (2015) 832–837.
[33] J. Rajagopalan, C. Rentenberger, H.P. Karnthaler, G. Dehm, M.T.A. Saif, Acta Mater. 58 (2010) 4772–4782.
[34] J. Rajagopalan, M.T.A. Saif, J. Mater. Res. 26 (2011) 2826–2832.
[35] J.H. Han, M.T.A. Saif, Rev. Sci. Instrum. 77 (2006), 045102.
[36] J.H. Han, J. Rajagopalan, M.T.A. Saif, Proc. SPIE 6464 (2007) 64640C.
[37] M.A. Haque, M.T.A. Saif, Exp. Mech. 42 (2002) 123–128.
[38] J. Williams, N. Chapman, N. Chawla, J. Elec. Mater. 42 (2013) 224–229.
[39] Kiyotaka Tsuji, Role of grain-boundary free energy & surface free energy for tin whisker growth, http://unicon.co.jp/business/pdf/data_rollofgrain.pdf (accessed 04/15/2016).
[40] K.N. Tu, Chih Chen, Albert T. Wu, J. Mater. Sci. Mater. Electron. 18 (2007) 269–281.
[41] M.W. Barsoum, E.N. Hoffman, R.D. Doherty, S. Gupta, A. Zavaliangos, Phys. Rev. Lett. 93 (2004) 206104.
[42] B.-Z. Lee, D.N. Lee, Acta Mater. 46 (1998) 3701–3714.
[43] U. Ray, I. Artaki, P.T. Vianco, IEEE Transactions on Components, Packaging, and Manufacturing Technology-Part A(Vol. IX. No. I) March 1995.
[44] Julia R. Greer, William D. Nix, Phys. Rev. B 73 (245410) (2006) 1–6.
[45] Z.W. Shan, Raja K. Mishra, S.A. Syed Asif, Oden L. Warren, Andrew M. Minor, Nat. Mater. 7 (2008) 115–119.
[46] Y. Kinoshita, N. Ohno, Key Eng. Mater. 626 (2015) 46–49.
[47] C. Shashank Kaira, Sudhanshu S. Singh, Antony Kirubanandham, Nikhilesh Chawla, Acta Mater. 120 (2016) 56–67.